ACCOUNTS of chemical research

Article

pubs.acs.org/accounts

Long-Lived Charge Separation and Applications in Artificial Photosynthesis

Shunichi Fukuzumi,*[,†,‡] Kei Ohkubo,[†] and Tomoyoshi Suenobu[†]

[†]Department of Material and Life Science, Graduate School of Engineering, Osaka University and ALCA, Japan Science and Technology Agency, Suita, Osaka 565-0871, Japan

[‡]Department of Bioinspired Science, Ewha Womans University, Seoul 120-750, Korea

CONSPECTUS: Researchers have long been interested in replicating the reactivity that occurs in photosynthetic organisms. To mimic the long-lived charge separations characteristic of the reaction center in photosynthesis, researchers have applied the Marcus theory to design synthetic multistep electron-transfer (ET) systems. In this Account, we describe our recent research on the rational design of ET control systems, based on models of the photosynthetic reaction center that rely on the Marcus theory of ET.

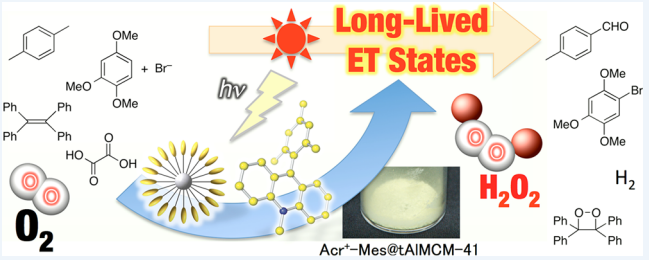

The key to obtaining a long-lived charge separation is the careful choice of electron donors and acceptors that have small reorganization energies of ET. In these cases, the driving force of back ET is located in the Marcus inverted region, where the lifetime of the charge-separated state lengthens as the driving force of back ET increases. We chose porphyrins as electron donors and fullerenes as electron acceptors, both of which have small ET reorganization energies. By linking electron donor porphyrins and electron acceptor fullerenes at appropriate distances, we achieved charge-separated states with long lifetimes. We could further lengthen the lifetimes of charge-separated states by mixing a variety of components, such as a terminal electron donor, an electron mediator, and an electron acceptor, mimicking both the photosynthetic reaction center and the multistep photoinduced ET that occurs there.

However, each step in multistep ET loses a fraction of the initial excitation energy during the long-distance charge separation. To overcome this drawback in multistep ET systems, we used designed new systems where we could finely control the redox potentials and the geometry of simple donor–acceptor dyads. These modifications resulted in a small ET reorganization energy and a high-lying triplet excited state. Our most successful example, 9-mesityl-10-methylacridinium ion (Acr^+–Mes), can undergo a fast photoinduced ET from the mesityl (Mes) moiety to the singlet excited state of the acridinium ion moiety (Acr^+) with extremely slow back ET. The high-energy triplet charge-separated state is located deep in the Marcus inverted region, and we have detected the structural changes during the photoinduced ET in this system using X-ray crystallography.

To increase the efficiency of both the light-harvesting and photoinduced ET, we assembled the Acr^+–Mes dyads on gold nanoparticles to bring them in closer proximity to one another. We can also incorporate Acr^+–Mes molecules within nanosized mesoporous silica–alumina. In contrast to the densely assembled dyads on gold nanoparticles, each Acr^+–Mes molecule in silica–alumina is isolated in the mesopore, which inhibits the bimolecular back ET and leads to longer lifetimes in solution at room temperature than the natural photosynthetic reaction center. Acr^+–Mes and related compounds act as excellent organic photocatalysts and facilitate a variety of reactions such as oxygenation, bromination, carbon–carbon bond formation, and hydrogen evolution reactions.

INTRODUCTION

The dependence of electron-transfer (ET) rate constants on thermodynamic and molecular dynamic parameters has been well-developed particularly in ET reactions of metal complexes involving redox active metal centers in light of the Marcus theory of ET, which provides basic principles to analyze the ET rate quantitatively.[1−3] According to the Marcus theory,[1] the rate constant of nonadiabatic intramolecular ET (k_{ET}) is given by eq 1, where V is the electronic coupling matrix element, h is the Planck constant, and T is the absolute temperature. In such a case, the logarithm of the ET rate constant ($\log k_{ET}$) is related parabolically to the ET driving force (negative ET free energy change) between electron donors and acceptors ($-\Delta G_{ET}$), and the ET reorganization energy (λ), that is, the energy required to structurally reorganize the donor, acceptor, and their solvation spheres upon ET. It is now well-recognized that the parabolic driving force dependence of $\log k_{ET}$ provides the theoretical basis for understanding ET processes in photosynthesis which is indispensable to our life.[1−3] There have been a variety of

$$k_{ET} = \left(\frac{4\pi^3}{h^2\lambda k_B T}\right)^{1/2} V^2 \exp\left[-\frac{(\Delta G_{ET} + \lambda)^2}{4\lambda K_B T}\right] \quad (1)$$

Received: August 13, 2013
Published: May 5, 2014

   dx.doi.org/10.1021/ar400200u | Acc. Chem. Res. 2014, 47, 1455−1464

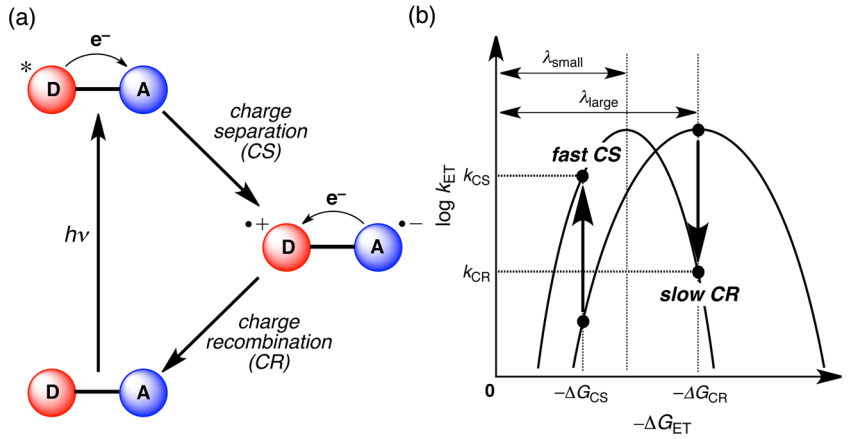

Figure 1. (a) Schematic diagram of photoinduced electron transfer of an electron donor–acceptor (D–A) dyad. (b) Driving force dependence of log k_{ET} with different λ values (for the meaning of λ, see text).

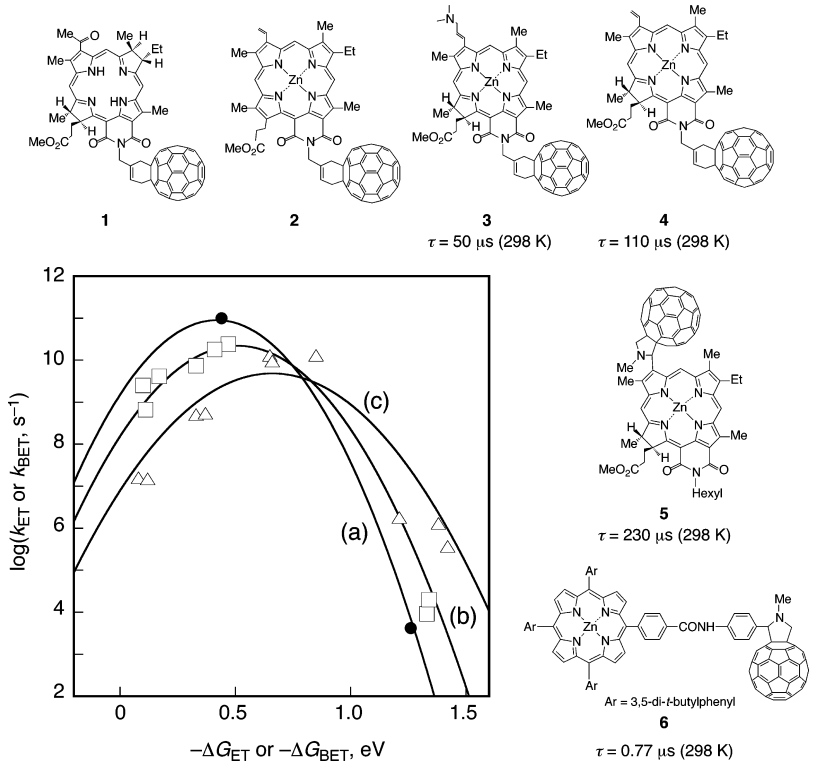

Figure 2. Electron donor–acceptor dyads of porphyrins, **2** and **6**; chlorines, **3**, **4**, and **5**; and a bacteriochlorin **1** with the CS lifetimes in PhCN and Marcus plots for (a) **5**, (b) **1**–**4**, and (c) **6**.[16–19]

excellent approaches to the application of the basic physical and chemical principles of photosynthesis to artificial systems.[4–11] Herein we describe our recent development of rational design to control ET systems, focusing on models of the photosynthetic reaction center in light of the Marcus theory of ET.

Rational Design to Mimic Photosynthetic Reaction Center

The primary step of photosynthesis is photoinduced ET from the singlet excited state of an electron donor (D) to an electron acceptor (A) in the D–A system (Figure 1a). The most important point for efficient energy conversion is to achieve the charge-separated (CS) state which has a sufficiently long lifetime for subsequent charge-separation steps in competition with the charge-recombination (CR) process to the ground state. According to the Marcus theory (eq 1),[1] the log k_{ET} value increases with increasing ET driving force ($-\Delta G_{ET}$) as shown in Figure 1b. When the magnitude of the driving force becomes the same as the reorganization energy ($-\Delta G_{ET} \sim \lambda$; Figure 1b), the reaction rate reaches a maximum and is basically controlled by the magnitude of electronic coupling (V) between the donor and acceptor moieties (eq 1). Upon passing this thermodynamic maximum, the highly exothermic region of the parabola ($-\Delta G_{ET} > \lambda$; Figure 1b) is entered, in which an additional increase of the driving force results in an actual slow-down of the reaction rate, due to an increasingly poor vibrational overlap of the product and reactant wave functions. This highly exergonic range is generally referred to as the Marcus *inverted* region.[1–3] In such a case the magnitude of the reorganization energy is the key parameter to control the ET process. The smaller the reorganization energy, the faster is the forward

dx.doi.org/10.1021/ar400200u | Acc. Chem. Res. 2014, 47, 1455–1464

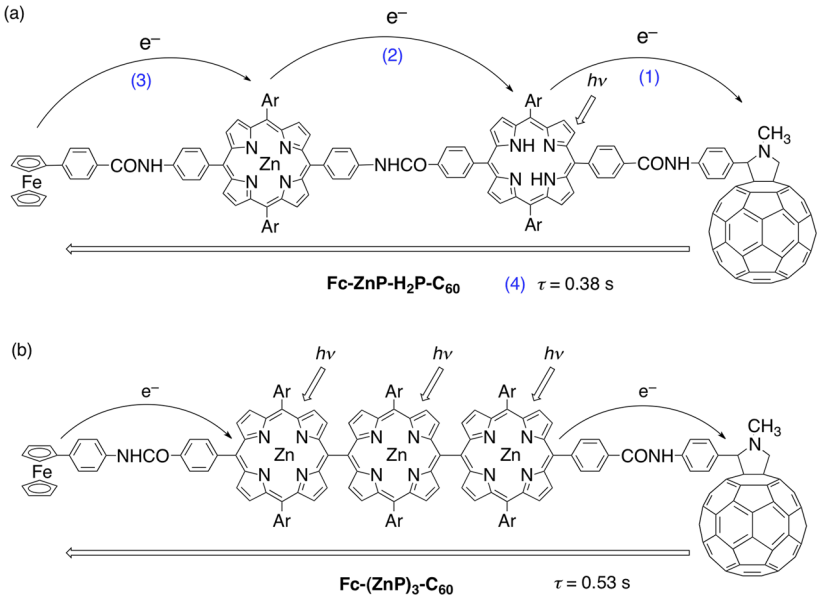

Figure 3. (a) Ferrocene–zinc porphyrin–free-base porphyrin–C_{60} tetrad (Fc–ZnP–H_2P–C_{60}) mimicking multistep charge separation in the photosynthetic reaction center. (1)–(3) denote the order of multistep electron transfer for the CS process and (4) is the CR process to the ground state. (b) Ferrocene–(*meso*,*meso*-linked porphyrin trimer)–fullerene pentad (Fc–$(ZnP)_3$–C_{60}). Ar = 3,5-Di-*tert*-butylphenyl.

photoinduced CS process, but the CR process becomes slower when the driving force for back ET ($-\Delta G_{ET}$) is larger than the ET reorganization energy (λ) as shown in Figure 1b. Thus, the CS lifetimes can be finely controlled by the λ value which is determined by the choice of the D and A pair, the type of linkage between the donor and acceptor molecules, and also the solvent. Extensive efforts have so far been made to achieve a long-lived CS state by tuning these factors.[4−13]

First, the choice of the donor–acceptor pair is of primary importance to design the artificial photosynthetic reaction center. Porphyrins which have highly delocalized π-systems are suitable for efficient ET because the uptake or release of electrons is associated with a small reorganization energy with minimal structural and solvation changes upon ET.[14] In the natural system, reduced porphyrins, namely, chlorins and bacteriochlorins, are the electron donor pigments of the ET processes. The number of reduced double bonds in the pyrrole rings is zero in the case of porphyrins, one in the case of chlorines, and two diagonal to each other in the case of bacteriochlorins (see Figure 2 for the structures of various porphyrinoids).

With the advent of fullerenes, fullerenes have been considered in general as an electron acceptor with small ET reorganization energies, which result from the large π-electron systems together with the rigid and confined structure composed only of carbon aromatic rings.[15] Thus, the combination of porphyrins- and chlorophyll-like donors with fullerene acceptors provides ideal donor–acceptor linked systems to achieve long-lived CS states. In this context, a series of free-base bacteriochlorin– and zinc chlorin–fullerene dyads as well as free-base porphyrin– and zinc porphyrin–fullerene dyads have been designed and synthesized as shown in Figure 2.[16−21]

The one-electron reduction potentials (E_{red}) of linked C_{60} in benzonitrile (PhCN) are almost invariant irrespective of the type of linked macrocyclic ring in **1**–**5** (Figure 2), whereas the one-electron oxidation potentials (E_{ox}) for oxidation of the macrocycles (**1**–**5**) are shifted in a negative direction in the following order: free-base porphyrin > free-base chlorin > zinc porphyrin > zinc chlorin.[16] Accordingly, the free energy change of ET from zinc chlorin (ZnCh) to C_{60} in **3**–**5** (equivalent to the driving force of the back ET), obtained from the difference between E_{ox} and E_{red}, is the smallest among the examined dyads. In this case, the radical ion pair state ($ZnCh^{\bullet+}$–$C_{60}^{\bullet-}$) in PhCN is lower in energy (1.33 eV) than both the triplet excited state of C_{60} (1.45 eV) and ZnCh (1.36–1.45 eV).[16] Thus, photoinduced ET from the singlet excited state of the ZnCh (^{1}ZnCh*) to the C_{60} moiety in the ZnCh–C_{60} dyad (**4**) occurs efficiently in PhCN with a rate constant of 2.4×10^{10} s^{-1} (lifetime of ^{1}ZnCh*, 41 ps) to produce the CS state ($ZnCh^{\bullet+}$–$C_{60}^{\bullet-}$) in competition with the intersystem crossing to ^{3}ZnCh* and energy transfer to produce ZnCh–$^1C_{60}$* and ZnCh–$^3C_{60}$*.[16] ET from ^{3}ZnCh* to C_{60} as well as ET from ZnCh to $^1C_{60}$* and $^3C_{60}$* also results in formation of $ZnCh^{\bullet+}$–$C_{60}^{\bullet-}$. In any case, the CS state ($ZnCh^{\bullet+}$–$C_{60}^{\bullet-}$) has been detected as a transient absorption spectrum (λ_{max} = 1000 nm due to $C_{60}^{\bullet-}$ and 790 nm due to $ZnCh^{\bullet+}$).[16]

The CS state ($ZnCh^{\bullet+}$–$C_{60}^{\bullet-}$) decays via back ET to the ground state rather than to the triplet excited state. The rate constant of back ET (k_{BET}) was determined from the disappearance of the absorption band at 790 nm due to $ZnCh^{\bullet+}$ of **4** as 9.1×10^3 s^{-1}, which corresponds to the CS lifetime of 110 μs.[16] The CS lifetime is highly sensitive to the substituents on the porphyrin ring and the type of linkage between the electron donor and acceptor (Figure 2).[17,19] Comparison of the CS lifetime of **6** with that of **4** is particularly intriguing. The CS energy of **6** is virtually the same as that of **4**. The main difference between **6** and **4** is the linkage length. The shorter linkage length of **4** than that of **6** results in a decrease in the solvent ET reorganization energy because of the smaller space between the donor and acceptor moieties for solvents to interact with the CS state.[17] As shown in Figure 1b, the smaller the λ value, the faster is the CS rate but slower becomes the CR rate, leading to the longer CS lifetime of **4** (110 μs) than that of **6** (0.77 μs).[17] This effect prevails over the larger V value with the shorter linkage length which would cause the faster ET rate.

dx.doi.org/10.1021/ar400200u | *Acc. Chem. Res.* 2014, 47, 1455–1464

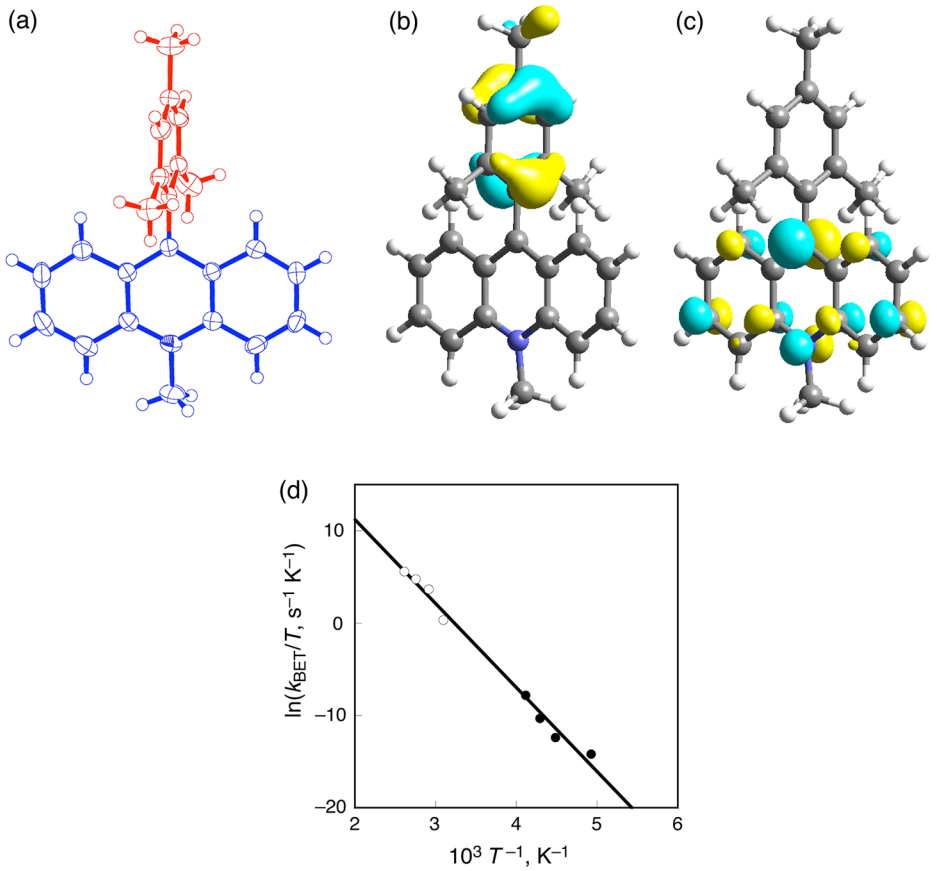

Figure 4. (a) Crystal structure of Acr^+–Mes. (b) HOMO and (c) LUMO calculated by a DFT method at the B3LYP/6-31G(d) level of theory. (d) Plot of $\ln(k_{BET}/T)$ vs T^{-1} for the intramolecular BET in $Acr^{\bullet}$–$Mes^{\bullet+}$ in PhCN determined by laser flash photolysis (○) and EPR (●) measurements.

The further decrease in the linkage length from **4** to **5** affords the longer CS lifetime (230 μs).[17,19]

The much slower CR process than the CS process in the D–A dyads in Figure 3 allows extension of the dyad systems to multistep ET systems by connecting additional donor and/or acceptor molecules to achieve a much longer lived CS state with a long linkage length between the terminal electron donor and acceptor.[20−22] Thus, a ferrocene–zinc porphyrin–free-base porphyrin–C_{60} tetrad (Fc–ZnP–H_2P–C_{60}) with the edge-to-edge distance of R_{ee} = 48.9 Å has been designed and synthesized as shown in Figure 3a.[20]

Energy transfer from ^{1}ZnP* (2.04 eV) to H_2P (1.89 eV) is followed by (1) ET from the singlet excited state of free-base porphyrin ($^1H_2P^*$) to C_{60} (see the arrow in Figure 3a). Then, (2) ET from ZnP to $H_2P^{\bullet+}$ occurs, followed by (3) the subsequent ET from Fc to $ZnP^{\bullet+}$ to yield the final CS state, Fc^+–ZnP–H_2P–$C_{60}^{\bullet-}$ (Figure 3a).[20] The lifetime of the resulting CS state at a long distance in a frozen PhCN has been determined as long as 0.38 s, and this is comparable to that observed for the bacterial photosynthetic reaction center, i.e., the lifetimes (∼ 1 s) of the bacteriochlorophyll dimer radical cation ($(Bchl)_2^{\bullet+}$)–secondary quinone radical anion ($Q_B^{\bullet-}$) ion pair.[22] Such an extremely long lifetime of a CS state could only be determined in frozen media, since in condensed media bimolecular back ET between two Fc^+–ZnP–H_2P–$C_{60}^{\bullet-}$ occurring at the diffusion-limited rate is much faster than the unimolecular CR process.[20]

An additional porphyrin moiety has been incorporated to construct the ferrocene–*meso*,*meso*-linked porphyrin trimer–fullerene pentad (Fc–$(ZnP)_3$–C_{60}) where the C_{60} and the ferrocene (Fc) are tethered at both the ends of $(ZnP)_3$ (R_{ee} = 46.9 Å; Figure 3b).[21] The lifetime of the final CS state (0.53 s at 163 K) has been prolonged without lowering the CS efficiency (Φ = 0.83).[21]

Rational Design To Achieve Much Longer Lifetime and Higher Energy Than That of the Natural Photosynthetic Reaction Center

The slow ET at a long distance has so far been utilized to attain the long-lived CS state, which is generated by multistep ET processes of molecular tetrads and pentads (*vide supra*). The synthesis of such compounds is extremely time-consuming, requiring a high cost. Moreover, a significant amount of energy is lost during the multistep ET processes to reach the final CS state. Thus, it is highly desired to design simple molecular dyads which are capable of fast charge separation but slow charge recombination. According to eq 1, the lifetime of the CS state of a simple molecular dyad (D–A) would increase with increasing the energy of the CS state, which corresponds to the driving force of back ET to the ground state, provided that the driving force of back ET is larger than the ET reorganization energy (Marcus inverted region). As mentioned above, however, the CS state energy should be lower than the triplet excited state of each component of D–A dyads. Otherwise the back ET would produce the triplet excited state rather than the ground state. Thus, we have designed and synthesized an electron donor–acceptor linked molecule with a small λ value and a high-lying triplet excited state.[23] Acridinium ion is the

dx.doi.org/10.1021/ar400200u | *Acc. Chem. Res.* 2014, 47, 1455−1464

best candidate for such a purpose, because the λ value for the electron self-exchange between the acridinium ion and the corresponding one-electron reduced radical is the smallest (0.3 eV) among the redox active organic compounds.[24] An electron donor moiety (mesityl group) is directly connected at the 9-position of the acridinium ion to yield 9-mesityl-10-methylacridinium ion (Acr^+−Mes), in which the solvent reorganization of ET is minimized because the overall charge (+1) remains the same in the charge-shift ET with a short linkage between the donor and acceptor moieties.[23] The X-ray crystal structure of Acr^+−Mes (Figure 4a) shows that the mesityl (donor) moiety is completely orthogonal to the acridinium ion (acceptor) moiety, indicating that there is no orbital interaction between the donor and acceptor moieties.[23] In addition, the density functional theory (DFT) calculation (B3LYP/6-31G(d) basis set) indicates that the highest occupied molecular orbital (HOMO) and lowest unoccupied molecular orbital (LUMO) are localized on the mesityl (donor) moiety and the acridinium ion (acceptor) moiety, as shown in Figure 4b,c, respectively.[23]

Irradiation of a deaerated PhCN solution of Acr^+−Mes by nanosecond laser excitation at 430 nm results in formation of the ET state ($Acr^{\bullet}$−$Mes^{\bullet+}$) via photoinduced ET from the mesitylene moiety to the singlet excited state of the acridinium ion moiety ($^1Acr^{+}$*−Mes) in PhCN at 298 K. The quantum yield of the ET state was determined as high as 98%.[23] The intramolecular back electron transfer (BET) of the ET state was too slow to compete with the intermolecular back ET reaction as in the case of Fc^+−ZnP−H_2P−$C_{60}^{\bullet-}$ (Figure 3a), since the decay time profile of $Acr^{\bullet}$−$Mes^{\bullet+}$ obeyed second-order kinetics.[23] In contrast, the decay of the ET state obeys first-order kinetics in PhCN at high temperatures (323−383 K).[23] This indicates that the rate of the *intra*molecular BET of the ET state becomes much faster than that of the *inter*molecular BET at higher temperatures because of the larger activation energy of the former than the latter as expected by eq 1.[23] The formation of the ET state is also detected by EPR under photoirradiation of Acr^+−Mes in frozen PhCN.[23] The disappearance of the EPR signal intensity obeyed first-order kinetics. The temperature dependence of the decay rate constant (k_{BET}) was also examined in frozen PhCN at 203−243 K.[23] The temperature dependence of k_{BET} in frozen PhCN at 203−243 K (Figure 4d, closed circles) falls on a single linear line with that in PhCN solution at 333−383 K (Figure 4d, open circles).[23] The CS lifetime is as long as 2 h at 203 K, becoming virtually infinite at 77 K.[23,25]

Such a long CS lifetime was questioned particularly in the case of 9-(1-naphthyl)-10-methylacridinium ion (Acr^+−NA), and the observed transient absorption spectrum in the microsecond time region was assigned to the locally excited triplet state due to the Acr^+ moiety, because the absorption band at 700 nm due to $NA^{\bullet+}$ was not observed.[26−28] However, the long CS lifetime of $Acr^{\bullet}$−$Mes^{\bullet+}$ at low temperature resulted from the triplet ET state rather than the locally excited triplet state as evidenced by the triplet EPR signal as discussed later.[29] It was also demonstrated that the singlet ET state ($Acr^{\bullet}$−$NA^{\bullet+}$) initially formed upon femtosecond laser excitation of Acr^+−NA was converted to the triplet π-dimer radical cation [($Acr^{\bullet}$−$NA^{\bullet+}$)(Acr^+−NA)] via an intermolecular reaction with Acr^+−NA in the microsecond time region, which exhibited a broad near-IR absorption at 1000 nm due to the π−π* transition of the dimer as shown in Figure 5a.[30,31] Formation of such a π-dimer radial cation of naphthalene was also observed in

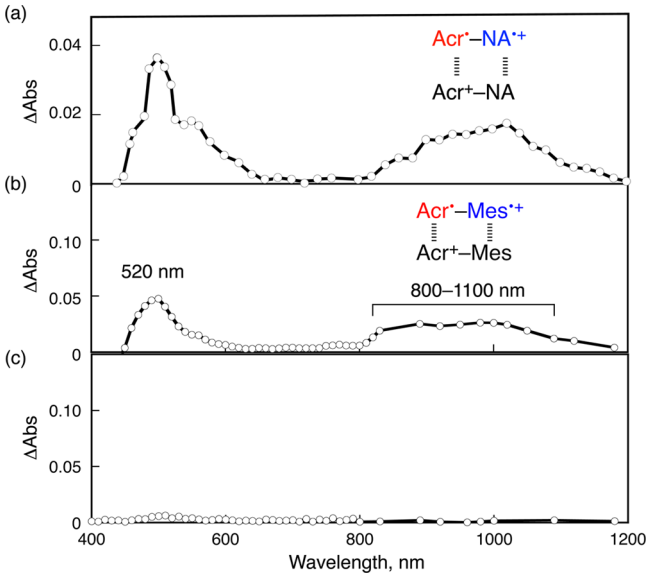

Figure 5. Transient absorption spectra of (a) Acr^+−NA (5.0×10^{-5} M), (b) Acr^+−Mes (2.0×10^{-5} M), and (c) Acr^+−Ph (2.0×10^{-5} M) in deaerated MeCN taken at 2.0 μs for a and 4.8 μs for both b and c after nanosecond laser excitation at 355 nm.

intermolecular photoinduced ET from naphthalene to the singlet excited state of unsubstituted $AcrH^+$.[30] Similarly, the π-dimer radical cation [($Acr^{\bullet}$−$Mes^{\bullet+}$)(Acr^+−Mes)] is observed as shown in Figure 5b.[30] In contrast to the cases of Acr^+−NA and Acr^+−Mes, no π-dimer radical cation was observed for Acr^+−Ph in which photoinduced ET from the Ph moiety to the Acr^+ moiety does not occur at all (Figure 5c).[30] The acridinium ion moiety can be replaced by a quinolinium ion in 2-phenyl-4-(1-naphthyl)quinolinium ion ($QuPh^+$−NA), which also afforded the π-dimer radical cation [($QuPh^{\bullet}$−$NA^{\bullet+}$)($QuPh^+$−NA)] of the ET state with a long lifetime.[31]

The long lifetime of the ET state of Acr^+−Mes has allowed us to observe the structural change in the Acr^+−Mes(ClO_4^-) crystal upon photoinduced ET directly by using laser pump and X-ray probe crystallographic analysis (Figure 6).[32] Upon photoexcitation of the crystal of Acr^+−Mes(ClO_4^-), the *N*-methyl group of the Acr^+ moiety was bent and its bending angle was 10.3(16)° when the *N*-methyl carbon moved 0.27(4) Å away from the mean plane of the ring as shown in Figure 6.[32] This bending is caused by the photoinduced ET from the Mes moiety to the Acr^+ moiety to produce $Acr^{\bullet}$−$Mes^{\bullet+}$, because the sp^2 carbon of the *N*-methyl group of Acr^+ is changed to the sp^3 carbon in the one-electron reduced state ($Acr^{\bullet}$).[32] The bending of the *N*-methyl group by photoexcitation was accompanied by the rotation and movement of the ClO_4^- by the electrostatic interaction with the $Mes^{\bullet+}$ moiety (Figure 6).[32] Thus, the observed bending of the *N*-methyl group and the movement of ClO_4^- provide strong evidence for the generation of the ET state of Acr^+−Mes upon photoexcitation. In contrast to the case of Acr^+−Mes, no geometrical difference was observed upon photoexcitation of Acr^+−Ph, which does not afford the ET state.[32]

Immobilization of Electron Donor−Acceptor Dyads

As previously described, photoexcitation of Acr^+−Mes affords the long-lived ET state ($Acr^{\bullet}$−$Mes^{\bullet+}$), which forms the π-dimer radical cation by an intermolecular reaction with Acr^+−Mes. In addition, intermolecular BET between the π-dimer radical

dx.doi.org/10.1021/ar400200u | Acc. Chem. Res. 2014, 47, 1455−1464

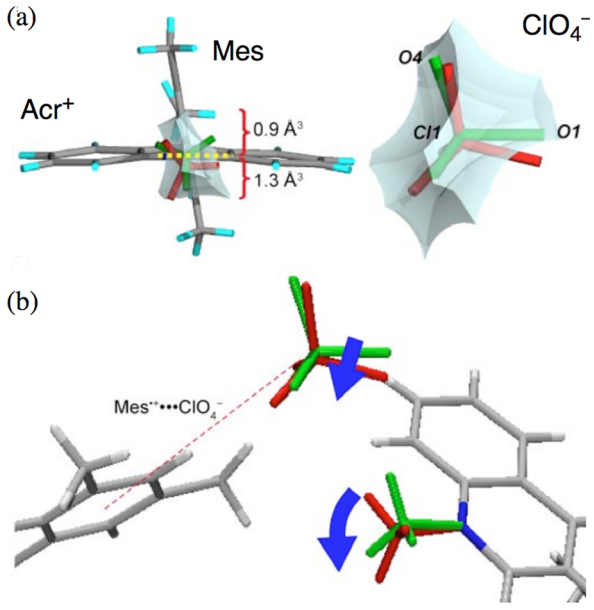

Figure 6. (a) Drawing of the reaction cavity (greenish-blue area): (left) drawing around the *N*-methyl group, with numbers indicating the volumes of the divided cavity formed by the yellow dotted line; (right) drawing around ClO_4^-. (b) Cooperative photoinduced geometrical changes. Fragments of the ground and ET state molecules are colored greenish-yellow and red, respectively. The red dashed line indicates the suggested $Mes^{\bullet+}\cdots ClO_4^-$ electrostatic interaction.

cations occurs in solution. In the natural photosynthesis, the photosynthetic reaction center is immobilized in chloroplast thylakoid membrane protein environments. Thus, it is interesting to immobilize Acr^+–Mes molecules.

First, Acr^+–Mes molecules were assembled on gold nanoparticles, by preparing 9-mesitylacridinium ion–monolayer-protected gold nanoclusters (Mes–Acr^+–PhS–AuC) as shown in Scheme 1.[33] Carboxyl-terminated Mes–Acr^+–COOH was directly coupled to 4-mercaptophenol-functionalized Au nanoclusters (PhS–AuC) in the presence of *N*,*N*′-diisopropylcarbodiimide (DIPC) and 4-(*N*,*N*-dimethylamino)pyridinium-4-toluenesulfonate (DPTS) as the standard coupling agents.[33] The mean diameter of the Au core was determined to be 1.7 ± 0.3 nm by transmission electron microscopy (TEM).[33] The amount of Mes–Acr^+ was determined to be 58 molecules per AuC (75% coverage) based on integration of the ^1H NMR signals due to the Mes–Acr^+ moiety.[33]

Femtosecond transient absorption spectroscopy of Mes–Acr^+–PhS–AuC with excitation at 420 nm revealed very rapid formation of π-dimer radical cation of the ET state of Mes–Acr^+ ($Mes^{\bullet+}$–$Acr^{\bullet}$–PhS–AuC) with neighboring Mes–Acr^+ as indicated by the broad transient near-IR band observed at 10 ps (Figure 7).[33] This indicates that the close proximity of Mes–

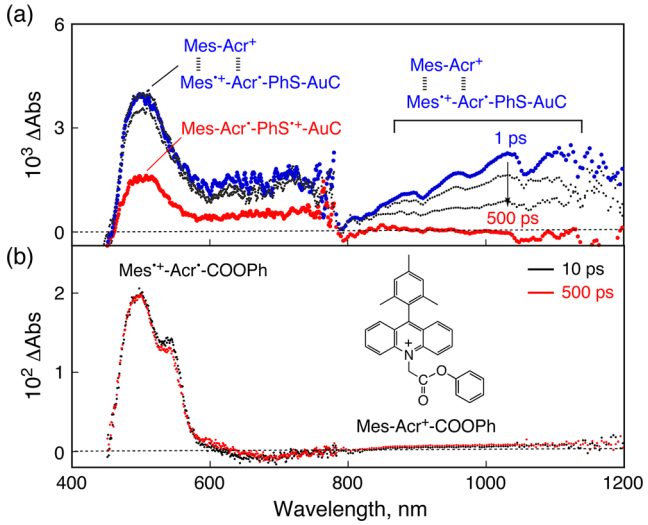

Figure 7. Transient absorption spectra observed in femtosecond laser flash photolysis (λ_{ex} = 420 nm) of (a) Mes–Acr^+–PhS–AuC at 1, 2, 3, and 500 ps and (b) Mes–Acr^+–COOPh at 10 and 500 ps in MeCN at 298 K.

Acr^+ molecules on AuC makes it possible to form the π-dimer radical cation via an intramolecular π–π interaction upon photoinduced ET from the Mes moiety to the singlet excited state of the Acr^+ moiety. In the case of the reference compound (Mes–Acr^+–COOPh), the transient absorption band at 490 nm due to the ET state of Mes–Acr^+–COOPh ($Mes^{\bullet+}$–$Acr^{\bullet}$–COOPh) is observed at 10 ps, whereas there is no transient absorption band in the near-IR region as shown in Figure 7.[33] However, the broad near-IR band appeared at 10 μs in nanosecond laser flash photolysis measurements. This indicates that the π-dimer radical cation of $Mes^{\bullet+}$–$Acr^{\bullet}$–COOPh with Mes–Acr^+–COOPh is formed by the intermolecular reaction,

Scheme 1

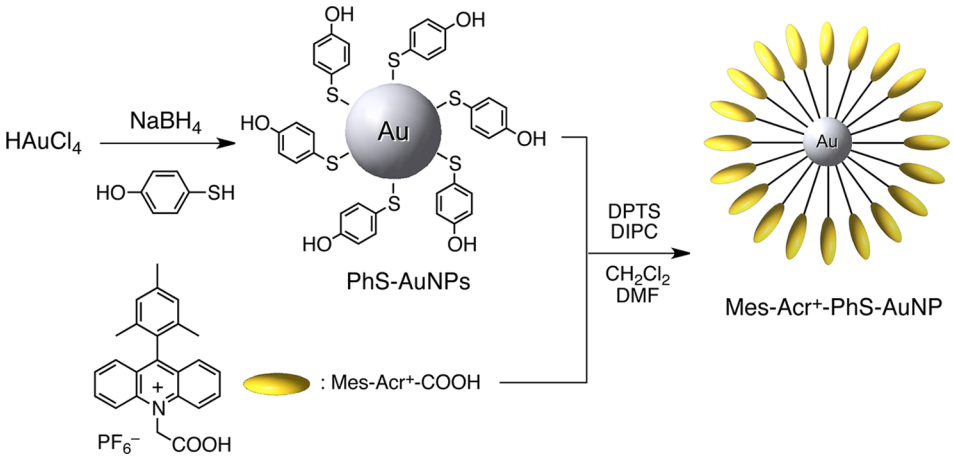

dx.doi.org/10.1021/ar400200u | *Acc. Chem. Res.* 2014, 47, 1455–1464

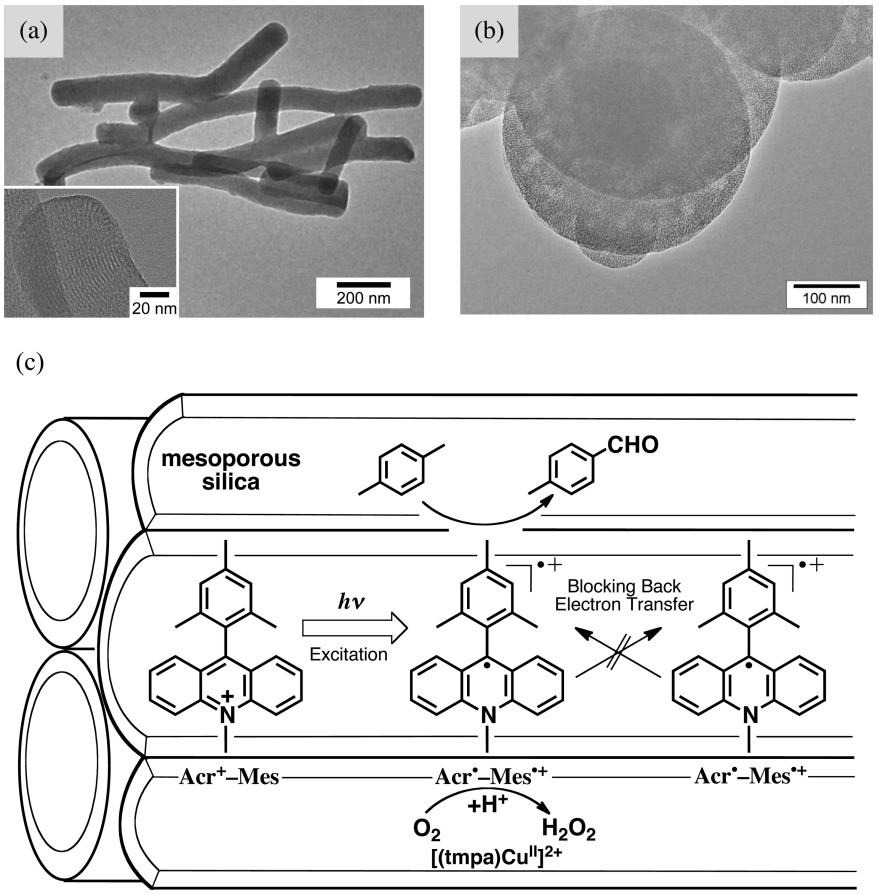

Figure 8. TEM images of (a) tAlMCM-41 and (b) sAlMCM-41 (the high-resolution image of tAlMCM-41 is inserted in a). (c) Reaction scheme of photocatalytic oxygenation of *p*-xylene with Acr^+–Mes and $[(tmpa)Cu^{II}]^{2+}$ incorporated into sAlMCM-41.

in sharp contrast to intramolecular formation of the π-dimer radical cation at 1 ps in Figure 7.[33]

Immobilization of Acr^+–Mes has also been achieved by incorporating Acr^+–Mes cation into nanosized mesoporous silica–alumina (AlMCM-41), which has cation exchange sites to obtain a nanocomposite (Acr^+–Mes@AlMCM-41).[29] The shape and size of nanosized AlMCM-41 were controlled by changing the preparation conditions as shown in Figure 8, where TEM images reveal a tubular or rodlike (tAlMCM-41) morphology in the diameter of 50–100 nm with the length of 0.2–2 μm array (part a) and also a sphere morphology (sAlMCM-41, part b).[29] The X-ray powder pattern of tAlMCM-41 exhibited a well-resolved pattern with a prominent peak (100) observed at ca. 2θ = 2.56°, indicating a highly ordered material with a hexagonal array.[29] Uniform channels with ca. 4 nm in diameter exist in a tube. Because the Acr^+–Mes molecular size is small enough as compared with the pore size of mesoporous silica with its diameter of more than 3 nm, cation exchange with Acr^+–Mes occurs spontaneously upon mixing Na^+-exchanged AlMCM-41 with Acr^+–Mes in acetonitrile.[29] The cation exchange percentages of tAlMCM-41 and sAlMCM-41 by Acr^+–Mes were determined to be 16% and 18%, respectively.[29] The incorporated Acr^+–Mes into AlMCM-41 was stable without leaching out in acetonitrile at room temperature.

Upon photoexcitation of Acr^+–Mes@tAlMCM-41 suspended in MeCN, photoinduced ET form the Mes moiety to the singlet excited state of the Acr^+ moiety occurred within 10 ps to produce the ET state as detected by laser flash photolysis and electron paramagnetic resonance (EPR) measurements.[29] In contrast to the case in solution (vide supra), no π-dimer radical cation was formed because each Acr^+–Mes molecule is isolated inside AlMCM-41.[29] The lifetime of the ET state of Acr^+–Mes@tAlMCM-41 suspended in acetonitrile was determined to be 2.3 s at 198 K, which is much longer than that in solution because of the inhibition of bimolecular BET in AlMCM-41 as illustrated in Figure 8.[29] Thus, incorporation of a simple electron donor–acceptor dyad into AlMCM-41 has made it possible to elongate the lifetime of the charge-separated state, which is longer than that of the bacterial photosynthetic reaction center (1 s).[22] The triplet ET state of $Acr^{\bullet}$–$Mes^{\bullet+}$@tAlMCM-41 was detected by an EPR spectrum measured at 4 K, which exhibited the fine structure together with a strong sharp signal at g = 4.0.[29] The distance between two electron spins was determined from the zero-field splitting parameters to be 7.7 Å, which agrees with the expected distance of 7.2 Å between an sp^2 carbon atom at the 4-position of the mesityl moiety and sp^2 carbon atoms at the 3- and 6-positions of the acridinyl moiety.[29] Polycondensation of Acr^+–Mes-bridged organosilane in the presence of a nonionic surfactant is also reported to yield a mesostructured organosilica solid with a functional framework that exhibited long-lived photoinduced charge separation.[34]

Photocatalysis of Long-Lived CS States

Since the long-lived ET state of Acr^+–Mes has the ability not only to oxidize an external electron donor but also to reduce an external electron acceptor, the photoirradiation of Acr^+–Mes in

dx.doi.org/10.1021/ar400200u | *Acc. Chem. Res.* 2014, 47, 1455–1464

the presence of D and A results in formation of the radical cation ($D^{\bullet+}$) and radical anion ($A^{\bullet-}$) at the same time, provided that the one-electron oxidation potential of D is less positive than the one-electron reduction potential of $Acr^{\bullet}$–$Mes^{\bullet+}$ (E_{red} = 1.88 V vs SCE) and that the one-electron reduction potential of A is more positive than the oxidation potential of $Acr^{\bullet}$–$Mes^{\bullet+}$ (E_{ox} = −0.49 V vs SCE).[23,35] Benniston et al. reported the photooxidation of the Mes moiety of Acr^{+}–Mes by oxygen.[36] However, even after 12 h photoirradiation of Acr^{+}–Mes with white light, only a small portion of Acr^{+}–Mes was oxidized by oxygen.[36] This indicates that Acr^{+}–Mes is rather photostable even in the presence of oxygen and that Acr^{+}–Mes can be used as an efficient organic photocatalyst.[36] Thus, formation of reactive radical cations and radical anions at the same time has enabled us and other groups to develop a variety of photocatalytic reactions with Acr^{+}–Mes.[35,37−42] It should be emphasized that the locally exited triplet state of Acr^{+}–Mes[26−28] would have no ability to reduce electron acceptors or to oxidize electron donors which have oxidation potentials higher than 1.4 V vs SCE. For example, visible light irradiation of the absorption band of Acr^{+}–Mes in an O_2-saturated acetonitrile (MeCN) solution containing tetraphenylethylene (TPE) results in formation of both $TPE^{\bullet+}$ and $O_2^{\bullet-}$, which are coupled by efficient 2 + 2 cycloaddition to yield the dioxetane (Scheme 2), which could

Scheme 2

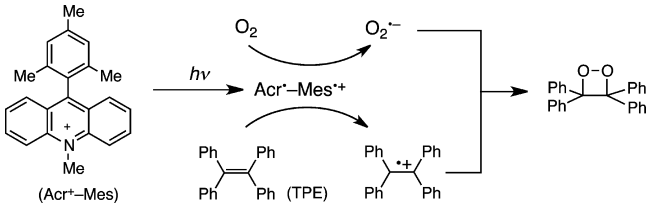

be obtained by the reaction of TPE with singlet oxygen, because singlet oxygen can react with only electron-rich alkenes.[43] When TPE was replaced by anthracene, 4 + 2 cycloaddition between anthracene radical cation and $O_2^{\bullet-}$ occurred efficiently to yield the corresponding endoperoxide (9,10-epidioxyanthracene).[44]

Selective photocatalytic oxygenation of *p*-xylene by O_2 to yield *p*-tolualdehyde and H_2O_2 at room temperature was made possible by using Acr^{+}–Mes as an organic photocatalyst.[45] No further oxygenated product, *p*-toluic acid or *p*-phthaladehyde, was produced during the photocatalytic reaction, because the $Mes^{\bullet+}$ moiety cannot oxidize *p*-tolualdehyde.[45] On the other hand, $O_2^{\bullet-}$ undergoes the disproportionation with proton to yield H_2O_2 and O_2.[45] The composite photocatalyst composed of Acr^{+}–Mes@sAlMCM-41 (vide supra) and [{tris(2-pyridylmethyl)amine}Cu^{II}]$^{2+}$ ([(tmpa)Cu^{II}]$^{2+}$) exhibited the highest catalytic activity and durability in the photocatalytic oxygenation of *p*-xylene with O_2.[33]

Acr^{+}–Mes can also act as an excellent organic photocatalyst for the oxidative bromination of aromatic compounds with HBr and O_2 (eq 2) at room temperature via addition of bromide

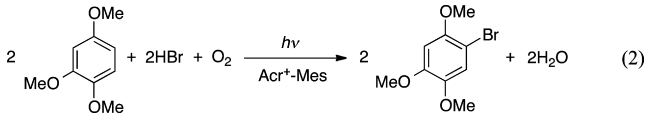

(2)

anion to radical cations of aromatic compounds produced by ET from aromatic compounds to the $Mes^{\bullet+}$ moiety of $Acr^{\bullet}$–$Mes^{\bullet+}$.[46] Efficient photocatalytic hydrogen evolution was also made possible using NADH and oxalic acids as electron donors and Acr^{+}–Mes or $QuPh^{+}$–NA as an organic catalyst with metal nanoparticles as hydrogen evolution catalysts.[47,48]

■ CONCLUSION AND PERSPECTIVE

Efficient multistep ET systems have been designed using suitable components based on the Marcus theory of ET to mimic the function of the photosynthetic reaction center. Rational design of simple molecular dyads capable of fast CS but extremely slow CR has significant advantages with regard to synthetic feasibility, providing a variety of applications in particular for development of efficient organic photocatalysts for oxygenation of substrates and hydrogen evolution from electron donors with metal nanoparticles. The incorporation of organic catalysts into nanosized mesoporous silica–alumina has enabled improvement of the photocatalytic reactivity and the durability. Such composite photocatalysts will be further combined with water-reduction and -oxidation catalysts as well as O_2-reduciton catalysts.

■ AUTHOR INFORMATION

Corresponding Author

*Tel.:+81-6-6879-7368. Fax: +81-6-6879-7370. E-mail: fukuzumi@chem.eng.osaka-u.ac.jp

Notes

The authors declare no competing financial interest.

Biographies

Shunichi Fukuzumi earned a Ph.D. degree in applied chemistry at Tokyo Institute of Technology in 1978. He has been a full professor of Osaka University since 1994. He is now a special distinguished professor at Osaka University.

Kei Ohkubo earned his Ph.D. degree in applied chemistry at Osaka University in 2001. He has been a designated associate professor at Osaka University since 2005.

Tomoyoshi Suenobu earned a Ph.D. degree in applied chemistry at Osaka University in 1994. He has been an assistant professor at Osaka University since 1994.

■ ACKNOWLEDGMENTS

We are most grateful to the collaborators and co-workers who performed the research reported in this Account and for support by a Grant-in-Aid from MEXT and an ALCA project from JST, Japan and KOSEF/MEST through the WCU Project (R31-2008-000-10010-0) and GRL (2010-00353) Program, Korea.

■ REFERENCES

(1) Marcus, R. A.; Sutin, N. Electron Transfers in Chemistry and Biology. *Biochem. Biophys. Acta* **1985**, *811*, 265−322.
(2) Barbara, P. F.; Meyer, T. J.; Ratner, M. A. Contemporary Issues in Electron Transfer Research. *J. Phys. Chem.* **1996**, *100*, 13148−13168.
(3) Gray, H. B.; Winkler, J. R. Electron Transfer in Proteins. *Annu. Rev. Biochem.* **1996**, *65*, 537−561.
(4) Gray, H. B. Powering the planet with solar fuel. *Nat. Chem.* **2009**, *1*, 7.
(5) Lewis, N. S.; Nocera, D. G. Powering the Planet: Chemical Challenges in Solar Energy Utilization. *Proc. Natl. Acad. Sci. U. S. A.* **2006**, *103*, 15729−15735.

(6) Gust, D.; Moore, T. A.; Moore, A. L. Solar Fuels via Artificial Photosynthesis. *Acc. Chem. Res.* **2009**, *42*, 1890−1898.
(7) Wasielewski, M. R. Self-Assembly Strategies for Integrating Light Harvesting and Charge Separation in Artificial Photosynthetic Systems. *Acc. Chem. Res.* **2009**, *42*, 1910−1921.
(8) Fukuzumi, S.; Ohkubo, K. Assemblies of Artificial Photosynthetic Reaction Centers. *J. Mater. Chem.* **2012**, *22*, 4575−4587.
(9) Guldi, D. M.; Sgobba, V. Carbon Nanostructures for Solar Energy Conversion Schemes. *Chem. Commun. (Cambridge, U. K.)* **2011**, *47*, 606−610.
(10) Fukuzumi, S.; Ohkubo, K.; D'Souza, F.; Sessler, J. L. Supramolecular Electron Transfer by Anion Binding. *Chem. Commun. (Cambridge, U. K.)* **2012**, *48*, 9801−9815.
(11) D'Souza, F.; Ito, O. Photosensitized Electron Transfer Processes of Nanocarbons Applicable to Solar Cells. *Chem. Soc. Rev.* **2012**, *41*, 86−96.
(12) Fukuzumi, S.; Kojima, T. Photofunctional Nanomaterials Composed of Multiporphyrins and Carbon-Based π-Electron Acceptor. *J. Mater. Chem.* **2008**, *18*, 1427−1439.
(13) Fukuzumi, S. Development of Bioinspired Artificial Photosynthetic Systems. *Phys. Chem. Chem. Phys.* **2008**, *10*, 2283−2297.
(14) Fukuzumi, S.; Endo, Y.; Imahori, H. A Negative Temperature Dependence of the Electron Self-Exchange Rates of Zinc Porphyrin π Radical Cations. *J. Am. Chem. Soc.* **2002**, *124*, 10974−10975.
(15) Guldi, D. M.; Fukuzumi, S. The Small Reorganization Energy of Fullerenes. In *Fullerenes: From Synthesis to Optoelectronic Properties*; Guldi, D. M., Martin, N., Eds.; Kluwer: Dordrecht, The Netherlands, 2003; pp 237−265.
(16) Fukuzumi, S.; Ohkubo, K.; Imahori, H.; Shao, J.; Ou, Z.; Zheng, G.; Chen, Y.; Pandey, R. K.; Fujitsuka, M.; Ito, O.; Kadish, K. M. Photochemical and Electrochemical Properties of Zinc Chlorin-C_{60} Dyad as Compared to Corresponding Free-Base Chlorin-C_{60}, Free-Base Porphyrin-C_{60}, and Zinc Porphyrin-C_{60} Dyads. *J. Am. Chem. Soc.* **2001**, *123*, 10676−10683.
(17) Ohkubo, K.; Imahori, H.; Shao, J.; Ou, Z.; Kadish, K. M.; Chen, Y.; Zheng, G.; Pandey, R. K.; Fujitsuka, M.; Ito, O.; Fukuzumi, S. Small Reorganization Energy of Intramolecular Electron Transfer in Fullerene-Based Dyads with Short Linkage. *J. Phys. Chem. A* **2002**, *106*, 10991−10998.
(18) Imahori, H.; Tamaki, K.; Guldi, D. M.; Luo, C.; Fujitsuka, M.; Ito, O.; Sakata, Y.; Fukuzumi, S. Modulating Charge Separation and Charge Recombination Dynamics in Porphyrin-Fullerene Linked Dyads and Triads: Marcus-Normal versus Inverted Region. *J. Am. Chem. Soc.* **2001**, *123*, 2607−2617.
(19) Ohkubo, K.; Kotani, H.; Shao, J.; Ou, Z.; Kadish, K. M.; Li, G.; Pandey, R. K.; Fujitsuka, M.; Ito, O.; Imahori, H.; Fukuzumi, S. Production of an Ultra-Long-Lived Charge-Separated State in a Zinc Chlorin-C_{60} Dyad by One-Step Photoinduced Electron Transfer. *Angew. Chem., Int. Ed.* **2004**, *43*, 853−856.
(20) Imahori, H.; Guldi, D. M.; Tamaki, K.; Yoshida, Y.; Luo, C.; Sakata, Y.; Fukuzumi, S. Charge Separation in a Novel Artificial Photosynthetic Reaction Center Lives 380 ms. *J. Am. Chem. Soc.* **2001**, *123*, 6617−6628.
(21) Imahori, H.; Sekiguchi, Y.; Kashiwagi, Y.; Sato, T.; Araki, Y.; Ito, O.; Yamada, H.; Fukuzumi, S. Long-Lived Charge-Separated State Generated in a Ferrocene-*meso*,*meso*-Linked Porphyrin Trimer-Fullerene Pentad with a High Quantum Yield. *Chem.—Eur. J.* **2004**, *10*, 3184−3196.
(22) Okamura, M. Y.; Feher, G. Proton-Coupled Electron Transfer Reactions of Q_B in Reaction Centers from Photosynthetic Bacteria. In *Anoxygenic Photosynthetic Bacteria*; Blankenship, R. E., Madigan, M. T., Bauer, C. E., Eds.; Kluwer: Dordrecht, The Netherlands, 1995; pp 577−594.
(23) Fukuzumi, S.; Kotani, H.; Ohkubo, K.; Ogo, S.; Tkachenko, N. V.; Lemmetyinen, H. Electron-Transfer State of 9-Mesityl-10-methylacridinium Ion with a Much Longer Lifetime and Higher Energy Than That of the Natural Photosynthetic Reaction Center. *J. Am. Chem. Soc.* **2004**, *126*, 1600−1601.
(24) Fukuzumi, S.; Ohkubo, K.; Suenobu, T.; Kato, K.; Fujitsuka, M.; Ito, O. Photoalkylation of 10-Alkylacridinium Ion via a Charge-Shift Type of Photoinduced Electron Transfer Controlled by Solvent Polarity. *J. Am. Chem. Soc.* **2001**, *123*, 8459−8467.
(25) Ohkubo, K.; Kotani, H.; Fukuzumi, S. Misleading Effects of Impurities Derived from Extremely Long-Lived Electron-Transfer State of 9-Mesityl-10-Methylacridinium Ion. *Chem. Commun. (Cambridge, U. K.)* **2005**, 4520−4522.
(26) Verhoeven, J. W.; van Ramesdonk, H. J.; Zhang, H.; Groeneveld, M. M.; Benniston, A. C.; Harriman, A. Long-Lived Charge-Transfer States in 9-Aryl-Acridinium Ions; A Critical Reinvestigation. *Int. J. Photoenergy* **2005**, *7*, 103−108.
(27) Benniston, A. C.; Harriman, A.; Li, P.; Rostron, J. P.; Verhoeven, J. W. Illumination of the 9-Mesityl-10-Methylacridinium Ion Does Not Give a Long-Lived Photoredox State. *Chem. Commun.(Cambridge, U. K.)* **2005**, 2701−2703.
(28) Benniston, A. C.; Harriman, A.; Li, P.; Rostron, J. P.; van Ramesdonk, H. J.; Groeneveld, M. M.; Zhang, H.; Verhoeven, J. W. Charge Shift and Triplet State Formation in the 9-Mesityl-10-methylacridinium Cation. *J. Am. Chem. Soc.* **2005**, *127*, 16054−16064.
(29) Fukuzumi, S.; Doi, K.; Itoh, A.; Suenobu, T.; Ohkubo, K.; Yamada, Y.; Karlin, K. D. Formation of a Long-Lived Electron-Transfer State in Nanosized Mesoporous Silica-Alumina Enhances Photocatalytic Oxidation Reactivity with a Copper Complex. *Proc. Natl. Acad. Sci. U. S. A.* **2012**, *109*, 15572−15577.
(30) Fukuzumi, S.; Kotani, H.; Ohkubo, K. Response: Why Had Long-lived Electron-Transfer States of Donor-Substituted 10-Methylacridinium Ions Been Overlooked? Formation of the Dimer Radical Cations Detected in the Near-IR Region. *Phys. Chem. Chem. Phys.* **2008**, *10*, 5159−5162.
(31) Kotani, H.; Ohkubo, K.; Fukuzumi, S. Formation of a Long-lived Electron-Transfer State of a Naphthalene-Quinolinium Ion Dyad and the π-Dimer Radical Cation. *Faraday Discuss.* **2012**, *155*, 89−102.
(32) Hoshino, M.; Uekusa, H.; Tomita, A.; Koshihara, S.; Sato, T.; Nozawa, S.; Adachi, S.; Ohkubo, K.; Kotani, H.; Fukuzumi, S. Structural Change upon Photoinduced Electron Transfer of a Donor−Acceptor Dyad Detected by X-ray. *J. Am. Chem. Soc.* **2012**, *134*, 4569−4572.
(33) Fukuzumi, S.; Hanazaki, R.; Kotani, H.; Ohkubo, K. Synthesis and Photodynamics of 9-Mesitylacridinium Ion-Modified Gold Nanoclusters. *J. Am. Chem. Soc.* **2010**, *132*, 11002−11003.
(34) Mizoshita, N.; Yamanaka, K.; Shimada, T.; Tania, T.; Inagaki, S. Mesostructured Organosilica with a 9-Mesityl-10-methylacridinium Bridging Unit: Photoinduced Charge Separation in the Organosilica Framework. *Chem. Commun. (Cambridge, U. K.)* **2010**, *46*, 9235−9237.
(35) Fukuzumi, S.; Ohkubo, K. Selective Photocatalytic Oxygenation Reactions with Organic Photocatalysts. *Chem. Sci.* **2013**, *4*, 561−574.
(36) Benniston, A. C.; Elliott, K. J.; Harrington, R. W.; Clegg, W. On the Photochemical Stability of the 9-Mesityl-10-methylacridinium Cation. *Eur. J. Org. Chem.* **2009**, 253−258.
(37) Nicewicz, D. A.; Nguyen, T. M. Recent Applications of Organic Dyes as Photoredox Catalysts in Organic Synthesis. *ACS Catal.* **2014**, *4*, 355−360.
(38) Wilger, D. J.; Gesmundo, N. J.; Nicewicz, D. A. Catalytic Hydrotrifluoromethylation of Styrenes and Unactivated Aliphatic Alkenes via an Organic Photoredox System. *Chem. Sci.* **2013**, *4*, 3160−3165.
(39) Perkowski, A. J.; Nicewicz, D. A. Direct Catalytic Anti-Markovnikov Addition of Carboxylic Acids to Alkenes. *J. Am. Chem. Soc.* **2013**, *135*, 10334−10337.
(40) Nguyen, T. M.; Nicewicz, D. A. Anti-Markovnikov Hydroamination of Alkenes Catalyzed by an Organic Photoredox System. *J. Am. Chem. Soc.* **2013**, *135*, 9588−9591.
(41) Grandjean, J.-M. M.; Nicewicz, D. A. Synthesis of Highly Substituted Tetrahydrofurans by Catalytic Polar-Radical-Crossover Cycloadditions of Alkenes and Alkenols. *Angew. Chem., Int. Ed.* **2013**, *52*, 3967−3971.

(42) Lee, S.; You, Y.; Ohkubo, K.; Fukuzumi, S.; Nam, W. Photoelectrocatalysis to Improve Cycloreversion Quantum Yields of Photochromic Dithienylethene Compounds. *Angew. Chem., Int. Ed.* **2012**, *51*, 13154−13158.
(43) Ohkubo, K.; Nanjo, T.; Fukuzumi, S. Efficient Photocatalytic Oxygenation of Tetraphenylethylene to Dioxetane with Oxygen via Electron Transfer. *Org. Lett.* **2005**, *7*, 4265−4268.
(44) Kotani, H.; Ohkubo, K.; Fukuzumi, S. Photocatalytic Oxygenation of Anthracenes and Olefins with Dioxygen via Selective Radical Coupling Using 9-Mesityl-10-methylacridinium Ion as an Effective Electron-Transfer Photocatalyst. *J. Am. Chem. Soc.* **2004**, *126*, 15999−16006.
(45) Ohkubo, K.; Mizushima, K.; Iwata, R.; Souma, K.; Suzuki, N.; Fukuzumi, S. Simultaneous Production of *p*-Tolualdehyde and Hydrogen Peroxide in Photocatalytic Oxygenation of *p*-Xylene and Reduction of Oxygen with 9-Mesityl-10-methylacridinium Ion Derivatives. *Chem. Commun. (Cambridge, U. K.)* **2010**, *46*, 601−603.
(46) Ohkubo, K.; Mizushima, K.; Fukuzumi, S. Selective Photocatalytic Aerobic Bromination with Hydrogen Bromide via an Electron-Transfer State of 9-Mesityl-10-methylacridinium Ion. *Chem. Sci.* **2011**, *2*, 715−722.
(47) Yamada, Y.; Miyahigashi, T.; Kotani, H.; Ohkubo, K.; Fukuzumi, S. Photocatalytic Hydrogen Evolution under Highly Basic Conditions by Using Ru Nanoparticles and 2-Phenyl-4-(1-naphtyl)quinolinium Ion. *J. Am. Chem. Soc.* **2011**, *133*, 16136−16145.
(48) Yamada, Y.; Miyahigashi, T.; Kotani, H.; Ohkubo, K.; Fukuzumi, S. Photocatalytic Hydrogen Evolution with Ni Nanoparticles by Using 2-Phenyl-4-(1-naphthyl)quinolinium ion as a Photocatalyst. *Energy Environ. Sci.* **2012**, *5*, 6111−6118.